Supporting Information

Aggregation-induced emission supramolecular organic framework (AIE SOF) gels constructed from tri-pillar[5]arene-based foldamer for ultrasensitive detection and separation of multi-analytes

Tai-Bao Wei,[a] Xiao-Qiang Ma,[a] Yan-Qing Fan,[a] Xiao-Mei Jiang,[a] Hong-Qiang Dong,[a] Qing-Yu Yang,[a] Yun-Fei Zhang,[a] Hong Yao,[a] Qi Lin*[a] and You-Ming Zhang[a,b]*

[a] Key Laboratory of Eco-functional Polymer Materials of the Ministry of Education, Key Laboratory of Eco-environmental Polymer Materials of Gansu Province, College of Chemistry and Chemical Engineering, Northwest Normal University, Lanzhou, 730070, China. *E-mail: weitaibao@126.com, linqi2004@126.com.

[b] College of Chemistry and Chemical Engineering, Lanzhou City University, Lanzhou, Gansu, 730070, China.

Supporting information:

Number of pages: 19 (1-19)

Number of Fig. and Table: 26 (Fig. S1-S24 and Table S1-S2)

Table of Contents

Experiments 1

Schemes S1. Synthetic route to compound **SPQ5**. 2

Schemes S2. Synthetic route to compound **DP**. 3

Fig. S1 ^{1}H NMR spectra of **Z1**. 4

Fig. S2 ^{1}H NMR spectra of **P5**. 5

Fig. S3 ^{1}H NMR spectra of **SPQ5**. 5

Fig. S4 ^{13}C NMR spectra of **SPQ5**. 6

Fig. S5 High-resolution ESI-MS spectra of **SPQ5**. 6

Fig. S6 ^{1}H NMR spectra of **Z2**. 7

Fig. S7 ^{1}H NMR spectra of **DP**. 7

Fig. S8 ^{13}C NMR spectra of **DP**. 8

Fig. S9 High-resolution ESI-MS spectra of **DP**. 8

Fig. S10 Partial ^{1}H NMR spectra (400 MHz, DMSO-d_6, 298 K) of (a) 1.04 × 10^{-2} M **SPQ5**; (b) 1.04 × 10^{-2} M **SPQ5** and 2.35 × 10^{-2} M **DP**; (c) 1.04 × 10^{-2} M **SPQ5** and 4.70 × 10^{-2} M **DP**; (d) 1.04 × 10^{-2} M **SPQ5** and 7.05 × 10^{-2} M **DP**. 9

Fig. S11 2D NOESY spectra of **SPQ5-DP** in DMSO-d_6 solution. 9

Fig. S12 High-resolution ESI-MS spectra of **SPQ5-DP**. 10

Fig. S13 FT-IR spectra of powder **SPQ5** and xerogel **FSOF**. 10

Fig. S14 Partial concentration-dependent ^{1}H NMR spectra (400MHz, DMSO-d_6, 298 K) of **SPQ5-DP**: (a) 2.07 × 10^{-3} M; (b) 4.18 × 10^{-3} M; (c) 1.03 × 10^{-2} M; (d) 1.66 × 10^{-2} M; (e) 2.07 × 10^{-2} M. 11

Fig. S15 The powder XRD patterns of **FSOF**, **FSOF-Fe** and **FSOF-Fe**+CN^-. 11

Fig. S16 The SEM images of xerogel powder (a) **SPQ5**; (b) **FSOF**. 12

Fig. S17 Multi-analytes response properties of **FSOF**. 12

Fig. S18 The powder XRD patterns of **FSOF**, **FSOF-Cr** and **FSOF-Cr**+$H_2PO_4^-$ 12

Fig. S19 The powder XRD patterns of **FSOF** and **FSOF-Hg**. 13

Fig. S20 (a) Emission spectra of **FSOF** with increasing amounts of Hg^{2+}; (b) photographs of the linear ranges **FSOF** for Hg^{2+}. 13

Fig. S21 Photographs of the linear ranges (a) **FSOF** for Fe^{3+}; (b) **FSOF** for Cr^{3+}; (c) **FSOF-Fe** for CN^-; (d) **FSOF-Cr** for $H_2PO_4^-$.....14

Fig. S22 FT-IR spectra of xerogel **FSOF**, **FSOF-Fe**, and **FSOF-Fe**+CN^-. 14

Fig. S23 FT-IR spectra of xerogel **FSOF**, **FSOF-Cr**, and **FSOF-Cr**+$H_2PO_4^-$. 15

Fig. S24 FT-IR spectra of xerogel **FSOF** and **FSOF-Hg**.....15

Table S1. Gelation Property of tri-pillar[5]arene-based foldamer supramolecular organic framework (**FSOF**). 16

Table S2. Comparison of **the** LODs and adsorption rates of different fluorescence sensors for ions.....17

References 18

Experiments

Materials and physical methods

All anions were used as tetrabutylammonium salts, which were purchased from Alfa Aesar and used as received. All metal ions were prepared from the perchlorate salts. Other reagents used in the study were of analytical grade. Fresh double distilled water was used throughout the experiment. All other reagents and solvents were commercially available at analytical grade and were used without further purification. ^{1}H NMR spectroscopy were recorded on Mercury-400BB spectrometer (600MHz) and Bruker Digital RF spectrometer (400MHz). ^{1}H chemical shifts are reported in ppm downfield from tetramethyl silane (TMS, TM scale with the solvent resonances as internal standards). Mass spectra were performed on a Bruker Esquire 3000 plus mass spectrometer (Bruker Franzen Analytik GmbH Bremen, Germany) equipped with ESI interface and ion trap analyzer. The X-ray diffraction analysis (XRD) was performed on a Rigaku D/Max-2400 X-Ray Diffractometer. The morphologies and sizes of the xerogel were characterized using field emission scanning electron microscopy (FE-SEM, JSM-6701F) at an accelerating voltage of 8 kV. The infrared spectra were performed on a Digiab FTS-3000 Fourier transform infrared spectrophotometer. Melting points were measured on an X-4 digital melting-point apparatus (uncorrected). Fluorescence spectra were recorded on a Shimadzu RF-5301PC spectrofluorophotometer.

Synthesis and characterizations of compound SPQ5

Synthesis of compound **Z1 (**1-(6-bromohexine)-4-methoxybenzene): In a 500 mL round-bottom flask, 4-methoxyphenol (2.48 g, 20 mmol), K_2CO_3 (8.28 g, 60 mmol), KI (9.96 g, 60 mmol), 1 6-dibromohexine (14.52 g, 60 mmol) and acetone (400 mL) were added. The mixture was heated reflux at 60 °C for 3 d (Schemes S1). After the solid was filtered off and the solvent was removed. Column chromatography (silica gel; petroleum ether: ethyl acetate = 20:1) afforded a white solid (5.4 g, 94%). M.P.:

87°C. ^{1}H NMR (600 MHz, $DCCl_3$, room temperature) (Fig. S1) δ (ppm): 6.81(s, 4H), 3.90(t, *J* = 4.4Hz, 4H), 3.42(t, *J* =4.8Hz, 4H), 1.89 (m, 4H), 1.77 (m, 4H), 1.49(t, J=2.4 Hz, 8H).

Synthesis of compound **P5** (pillar[5]arene): 1-(6-dibromohexne)- 4-methoxybenzene (1.44 g, 5 mmol) and 1, 4-dimethoxybenzene (5.40 g, 25 mmol) in 1, 2-dichloroethane (250 mL), paraformaldehyde (0.75 g, 25 mmol) was added. Then, boron trifluoride diethyl etherate ($BF_3{\cdot}O(C_2H_5)_2$, 5 mL, 47.0%-47.7%) was added to the solution and the mixture was stirred at 30°C for 30 min (Schemes S1). The solution was poured into water (150 mL) to quench the reaction. The mixture was extracted and the aqueous layer was removed. The organic layer was dried over anhydrous Na_2SO_4 and evaporated to afford the crude product, which was isolated by column chromatography using petroleum ether/Dichloromethane/ethyl acetate (v/v/v 100:25:1) to give **P5** as a white solid (2.08g, 39.62%).Mp: 191-194℃. ^{1}H NMR (Fig. S2) (600 MHz, $CDCl_3$) δ 6.78-6.74(m, 10H), 4.17-4.12 (t, *J* = 7.2Hz 2H), 3.81-3.71 (m, 10H), 3.82-3.65 (m, 27H), 2.62-2.58 (m, 2H), 1.79-1.74 (m, 2H), 1.55-1.49 (m, 4H), 1.27-1.22(m, 2H).

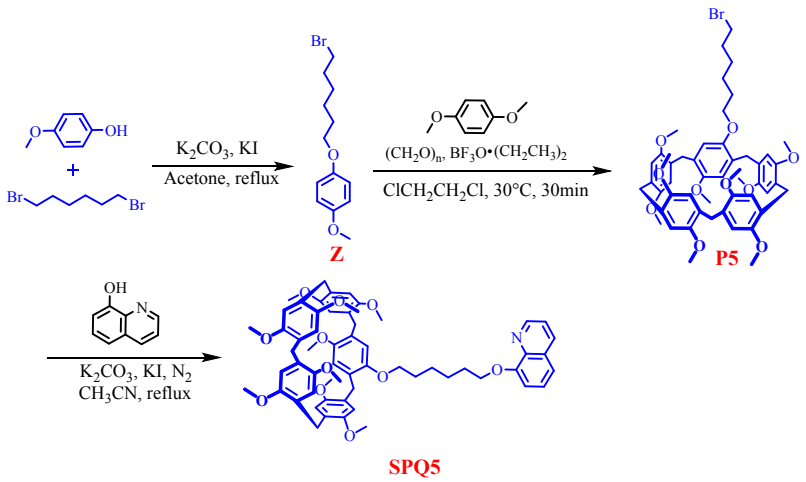

Schemes S1. Synthetic route to compound **SPQ5**.

Synthesis of **SPQ5:** Pillar[5]arene **P5** (0.90 g, 1 mmol) and KI (0.18 g, 1.1 mmol) were added to a solution of K_2CO_3 (0.14 g, 1 mmol) and 8-hydroxyquinoline(0.16 g, 1.1 mmol) in acetonitrile. The mixture was heated under nitrogen atmosphere at reflux for 48 h (Schemes S1). The solid was filtered off and the solvent was removed. The

crude product was isolated by column chromatography using petroleum ether/ethyl acetate (v/v 5:1) to get a white solid **SPQ5** (0.63, 65.35%). m.p. 92-94℃. ^{1}H NMR (Fig. S3) (600 MHz, $CDCl_3$, roomtemperature) δ (ppm): 8.95 (dd, *J*=4.2, 1H), 8.12 (dd, *J*=8.3, 1.6, 1H), 7.46-7.40 (m, 2H), 7.38 (dd, *J*=8.2, 0.8, 1H), 7.06 (d, *J*=7.7, 1H), 6.81-6.76 (m, 10H), 4.27 (t, *J*=6.9, 2H), 3.86 (t, *J*=6.5, 2H), 3.76 (dd, *J*=10.5, 6.3, 10H), 3.68-3.64 (m, 27H), 2.10-2.05 (m, 2H), 1.86 (dd, *J*=13.2, 6.7, 2H), 1.64 (dt, *J*=7.2, 3.5, 4H). ^{13}C NMR (Fig. S4) (151 MHz, $CDCl_3$) δ/ppm: 155.04, 150.85, 150.84, 150.20, 149.54, 140.64, 136.11, 129.74, 128.57, 128.44, 128.36, 126.89, 121.76, 119.69, 115.01, 114.11, 114.01, 108.84, 77.58, 77.27, 76.95, 69.03, 68.57, 55.91, 55.30, 31.13, 30.07, 29.75, 29.55, 29.25, 26.46, 26.31. ESI-MS m/z: [SPQ5] Calcd $C_{59}H_{65}N_1O_{11}$ 964.4639, found 964.4591 (Fig. S5).

Synthetic of compound **Z2**: 1, 6-dibromohexine (24.39 g, 100 mmol) and KI (13.28 g, 80 mmol) were added to a solution of K_2CO_3 (5.52 g, 40 mmol) and hydroquinone (2.20 g, 20 mmol) in acetone (300 mL). The mixture was heated under nitrogen atmosphere at reflux at 60 °C for 3 days (Scheme S2). The solid was filtered off and the solvent was removed. The residue was recrystallized in dichloromethane and petroleum ethers. The product **Z2** was collected by filtration, and dried under vacuum (8.12 g, 93.21%). M.P.: 85°C. ^{1}H NMR (Fig. S6) (600 MHz, $CDCl_3$, room temperature) δ 6.81 (s, 4H), 3.90 (t, 4H), 3.42 (t, 4H), 1.89 (m, 4H), 1.77 (m, 4H), 1.49 (m, 8H).

Synthesis of compound **DP**

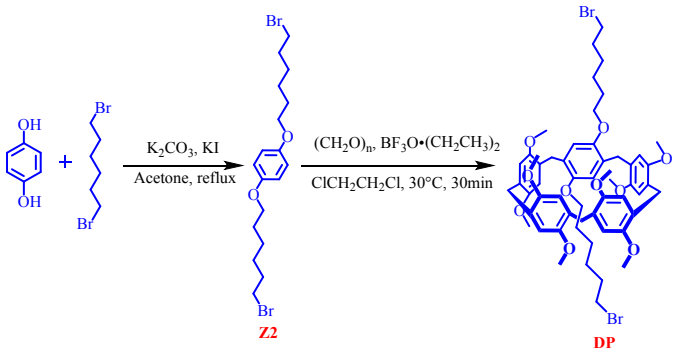

Schemes S2. Synthetic route to compound **DP**.

To a solution of 1, 4-dimethoxybenzene (4.14 g, 30 mmol) and **Z2** (1.89 g, 5 mmol) in 1, 2-dichloroethane (250 mL) was added paraformaldehyde (0.75 g, 25 mmol). Then, $BF_3O\cdot(C_2H_5)_2$ (4.5 ml, 36 mmol) was added to the solution, and the mixture was stirred at 30°C for 30 min (Scheme S2). The solution was poured into water (100 mL) to quench the reaction. The mixture was filtered and the solvent was removed. The residue was dissolved in dichloromethane. The organic layer was dried over anhydrous Na_2SO_4 and evaporated to afford the crude product, which was isolated by column chromatography using petroleum ether/dichloromethane/ethyl acetate (100:50:1) to give **DP** as a white solid (2.19 g, 41.98%). M.P.:188 °C. ^{1}H NMR (Fig. S7) (600 MHz, $CDCl_3$, room temperature) δ (ppm): 6.93(m, 10H), 3.82(m, 34H), 3.69(s, 4H), 1.49(m, 16H), 0.87(m, 4H). ^{13}C NMR (Fig. S8) ($CDCl_3$, 151 MHz), δ/ppm: 150.56, 150.40, 150.32, 150.22, 150.12, 149.54, 128.39, 128.23, 128.08, 127.90, 127.83, 114.60, 113.91, 113.27, 113.19, 113.08, 68.10, 55.69, 55.36, 55.26, 33.62, 31.56, 29.30, 29.27, 29.24, 29.15, 29.08, 27.59. HR-MS m/z: $[DP+NH_4]^+$ Calcd $C_{55}H_{68}O_{10}Br_2$ 1066.3497, found 1066.3496 (Fig. S9).

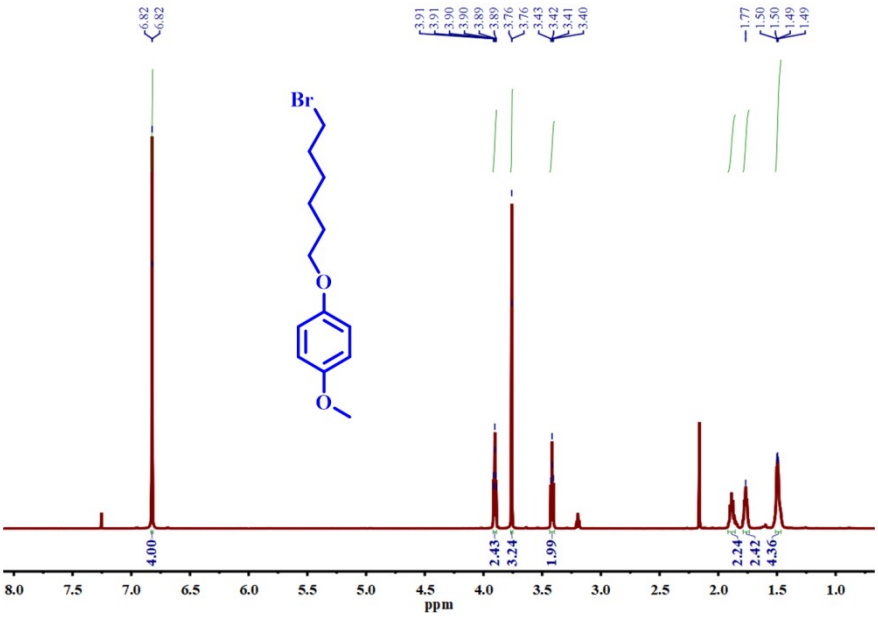

Fig. S1 ^{1}H NMR spectra of **Z1**.

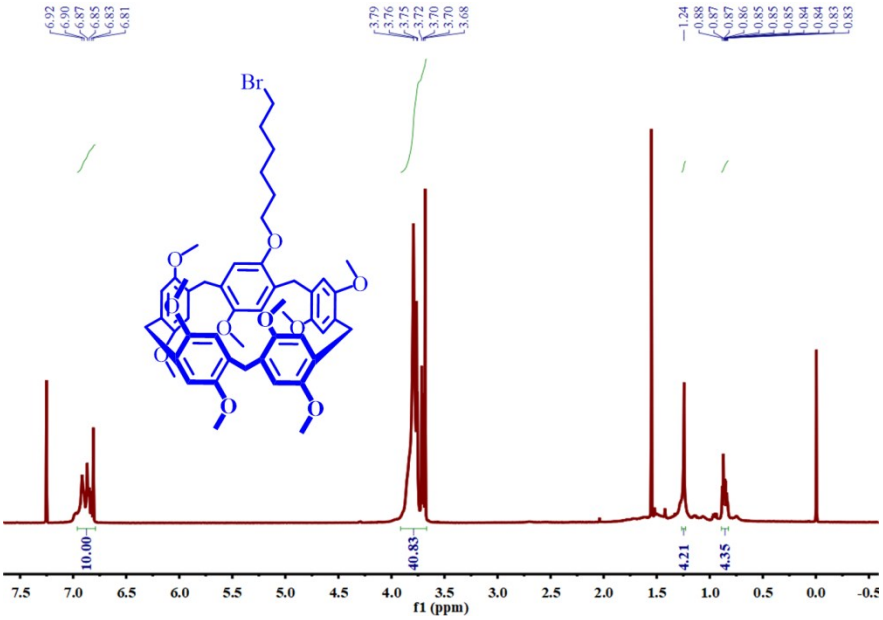

Fig. S2 ^{1}H NMR spectra of **P5**.

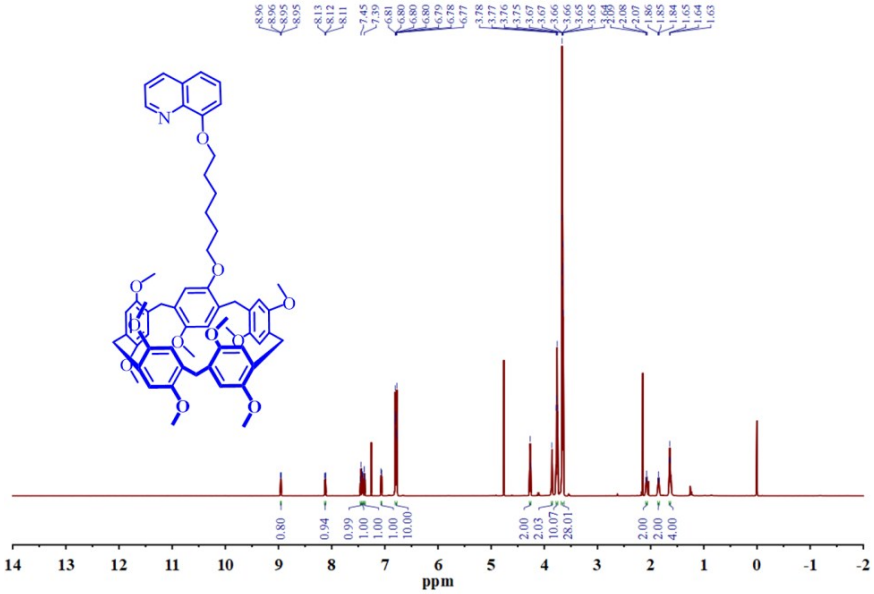

Fig. S3 ^{1}H NMR spectra of **SPQ5**.

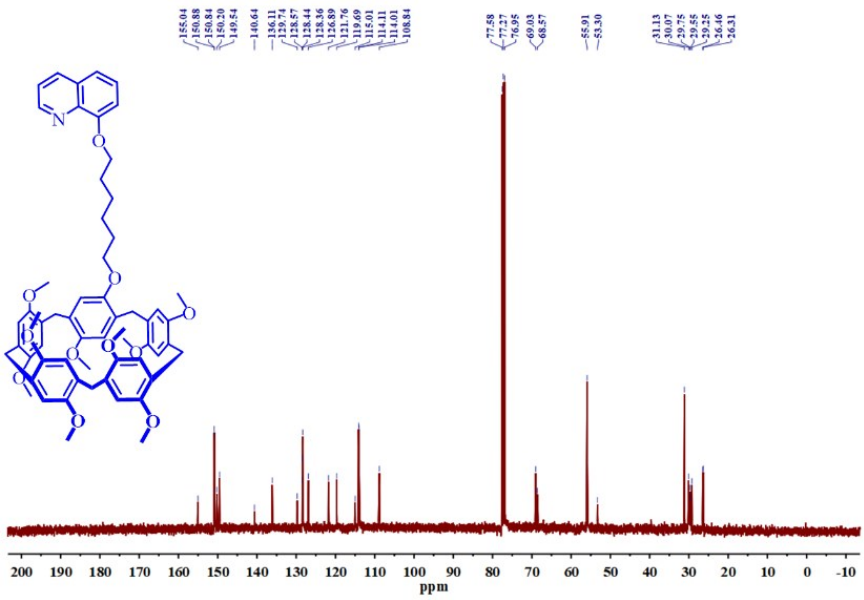

Fig. S4 ^{13}C NMR spectra of **SPQ5**.

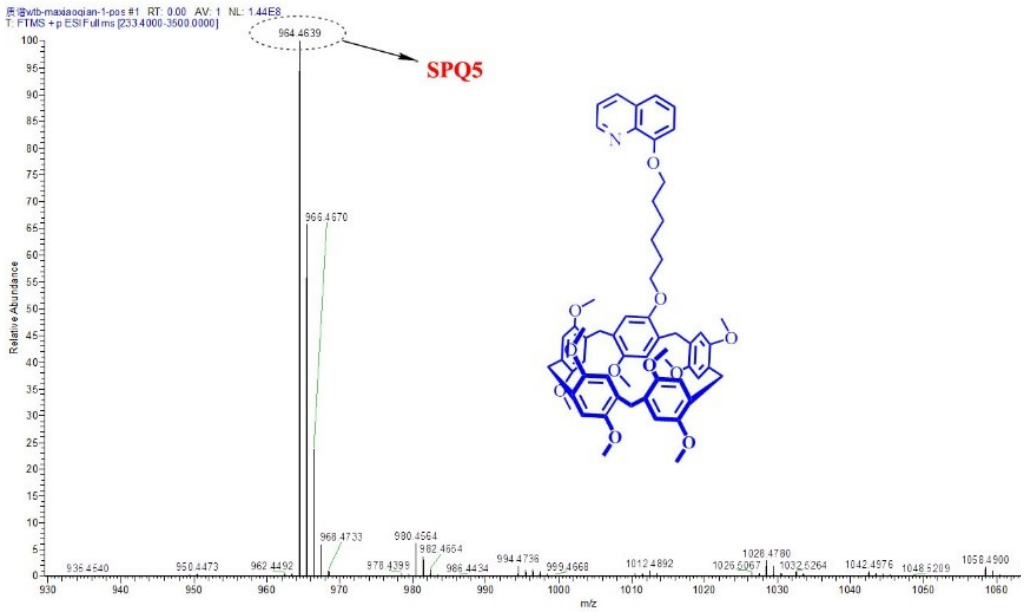

Fig. S5 High-resolution ESI-MS spectra of **SPQ5**.

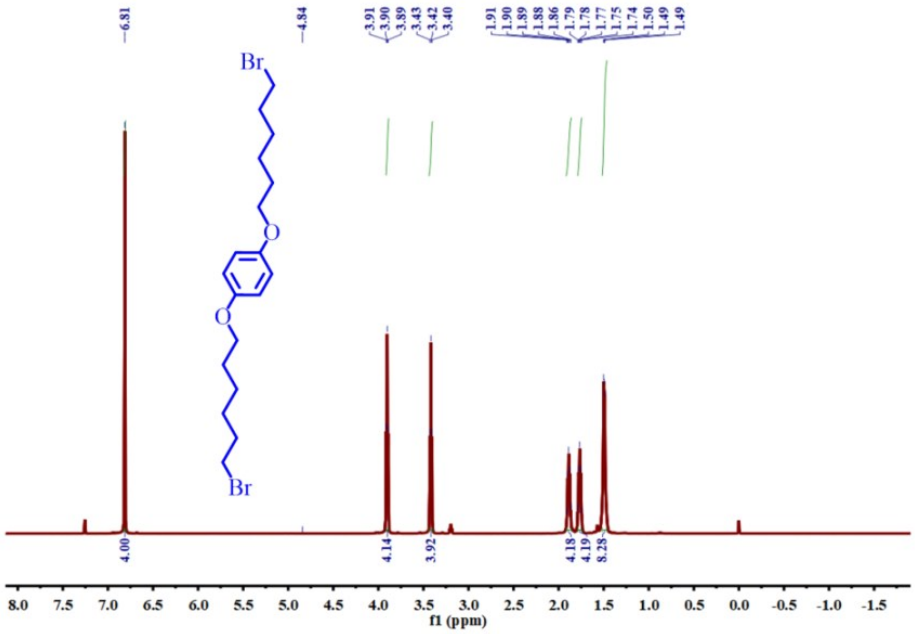

Fig. S6 ^{1}H NMR spectra of **Z2**.

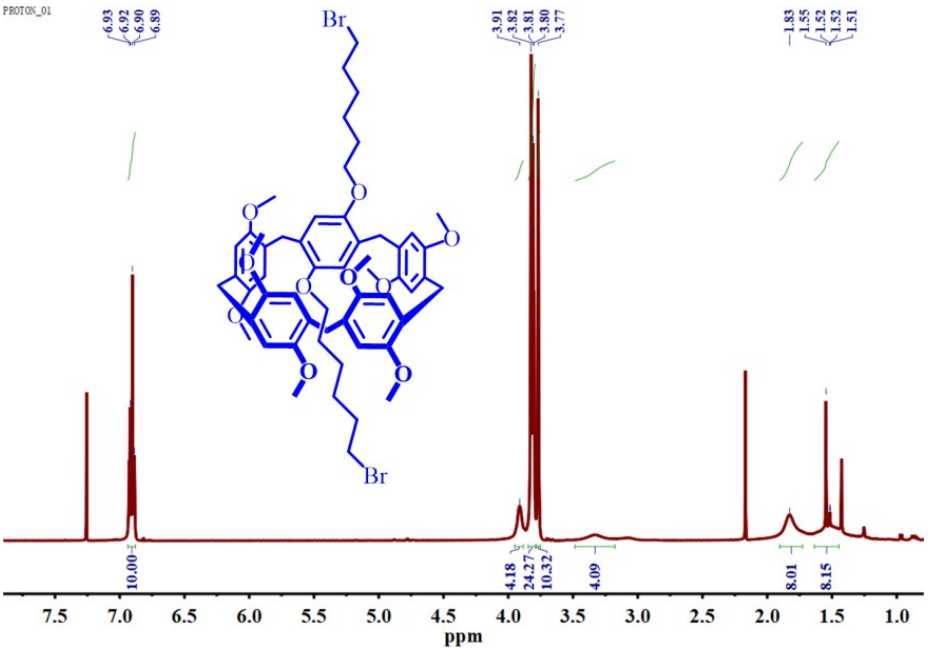

Fig. S7 ^{1}H NMR spectra of **DP**.

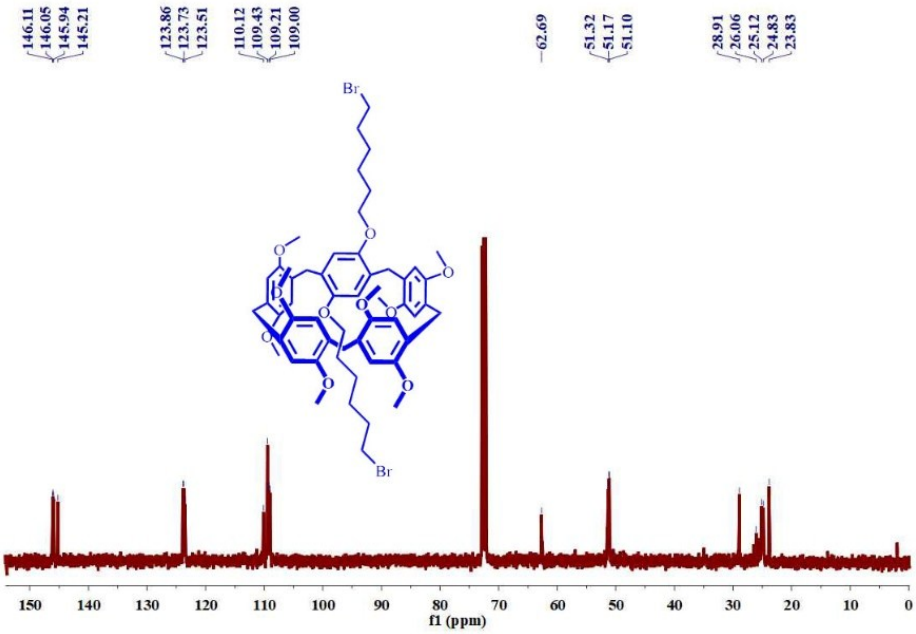

Fig. S8 ^{13}C NMR spectra of **DP**.

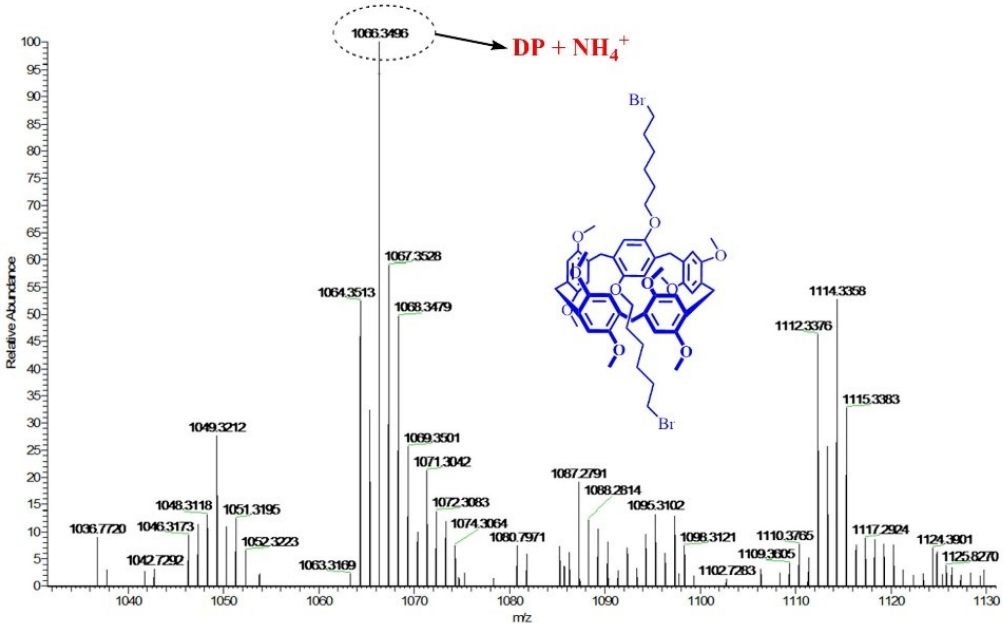

Fig. S9 High-resolution ESI-MS spectra of **DP**.

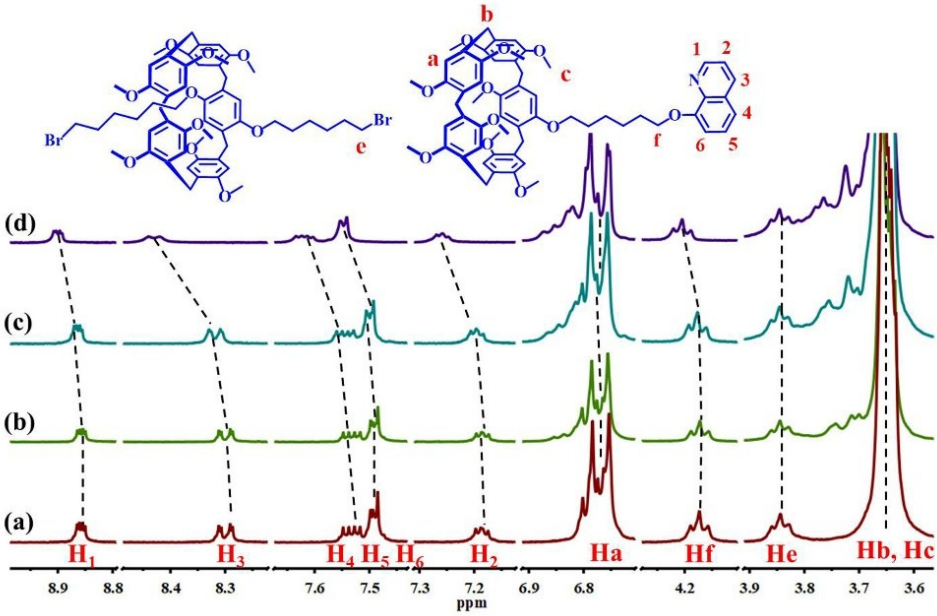

Fig. S10 Partial ^{1}H NMR spectra (400 MHz, DMSO-d_6, 298 K) of (a) 1.04 × 10^{-2} M **SPQ5**; (b) 1.04 × 10^{-2} M **SPQ5** and 2.35 × 10^{-2} M **DP**; (c) 1.04 × 10^{-2} M **SPQ5** and 4.70 × 10^{-2} M **DP**; (d) 1.04 × 10^{-2} M **SPQ5** and 7.05 × 10^{-2} M **DP**.

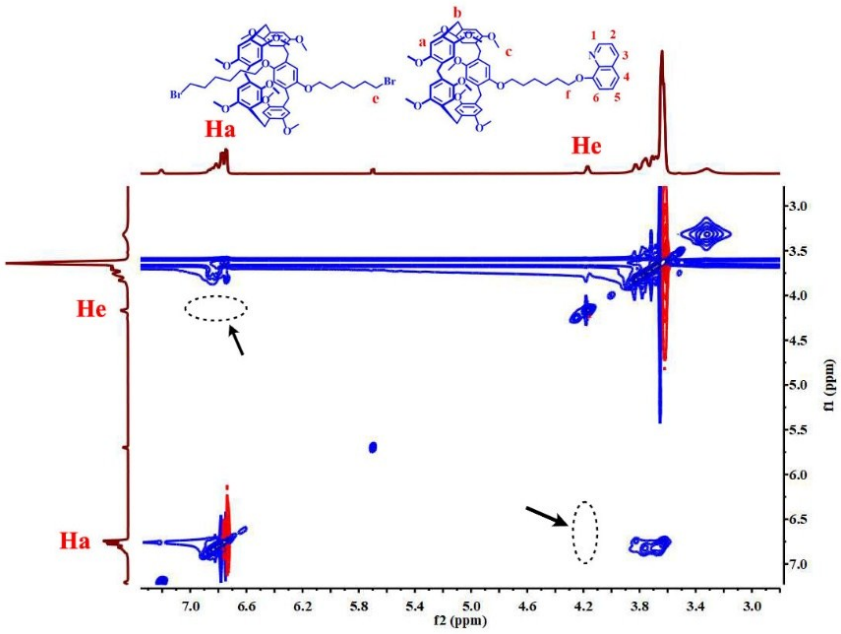

Fig. S11 2D NOESY spectra of **SPQ5-DP** in DMSO-d_6 solution.

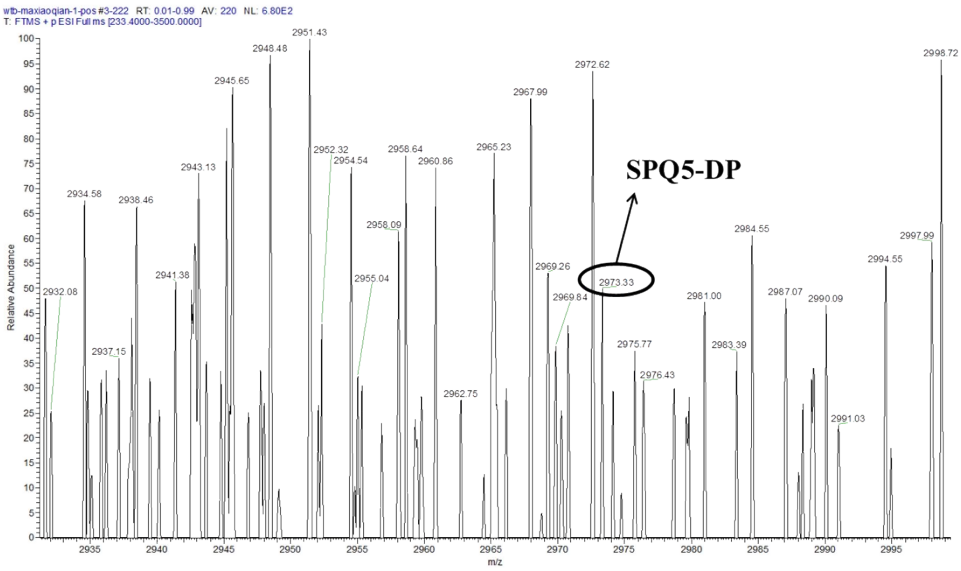

Fig. S12 High-resolution ESI-MS spectra of **SPQ5-DP**.

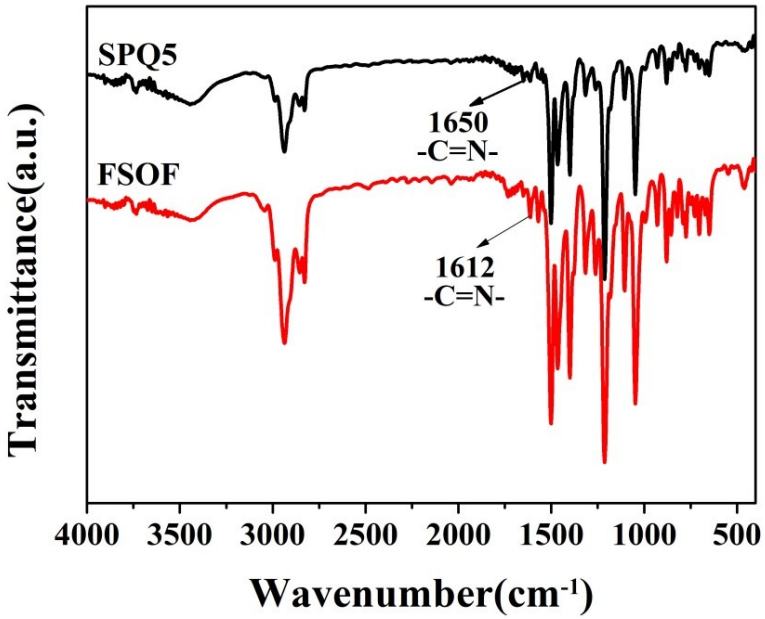

Fig. S13 FT-IR spectra of powder **SPQ5** and xerogel **FSOF**.

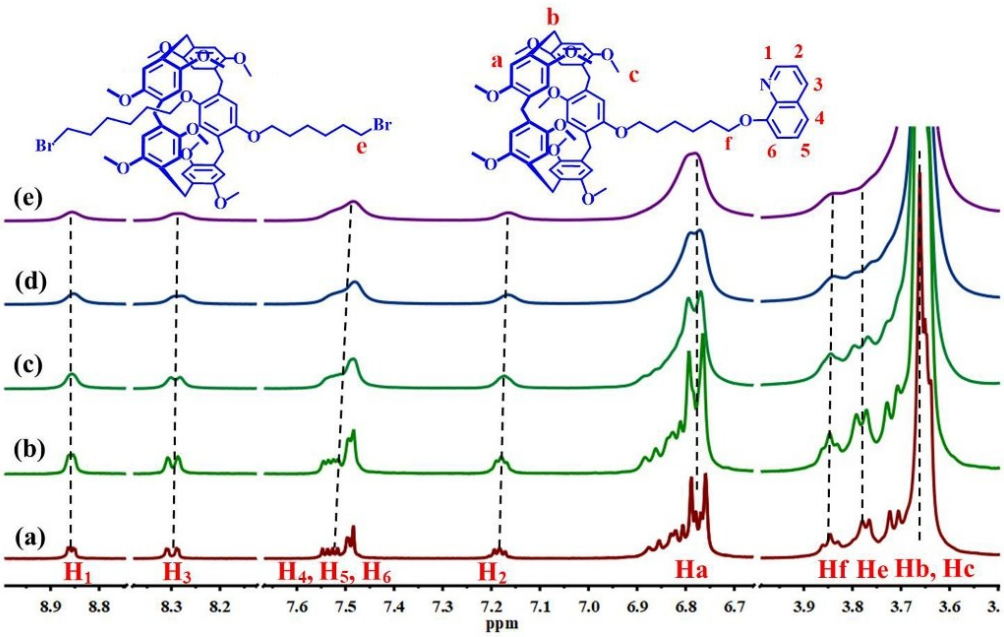

Fig. S14 Partial concentration-dependent ^{1}H NMR spectra (400MHz, DMSO-d_6, 298 K) of **SPQ5-DP**: (a) 2.07 × 10^{-3} M; (b) 4.18 × 10^{-3} M; (c) 1.03 × 10^{-2} M; (d) 1.66 × 10^{-2} M; (e) 2.07 × 10^{-2} M.

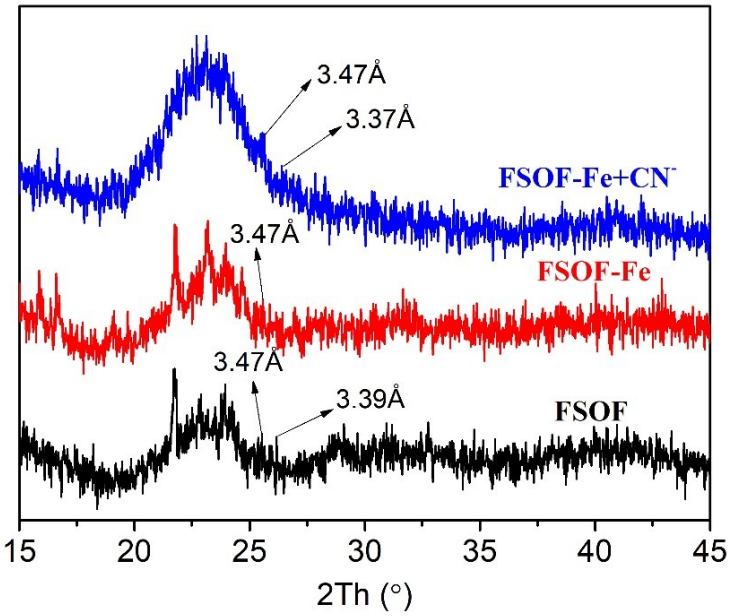

Fig. S15 The powder XRD patterns of **FSOF**, **FSOF-Fe** and **FSOF-Fe**+CN^-.

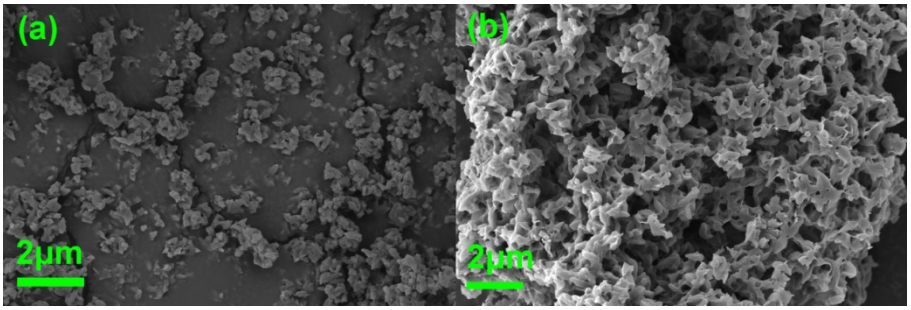

Fig. S16 The SEM images of xerogel powder (a) **SPQ5**; (b) **FSOF**.

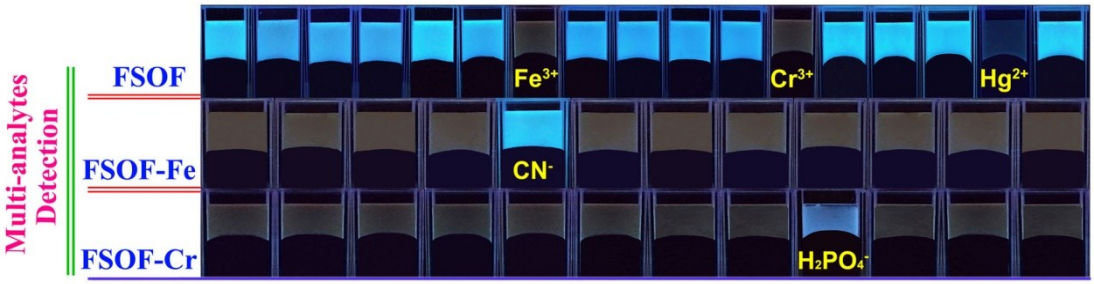

Fig. S17 Multi-analytes response properties of **FSOF**.

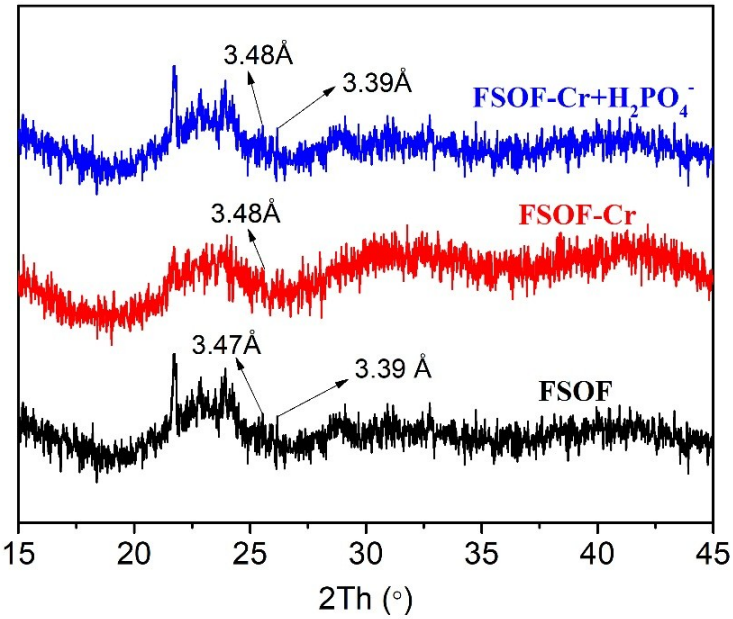

Fig. S18 The powder XRD patterns of **FSOF**, **FSOF-Cr** and **FSOF-Cr**+$H_2PO_4^-$

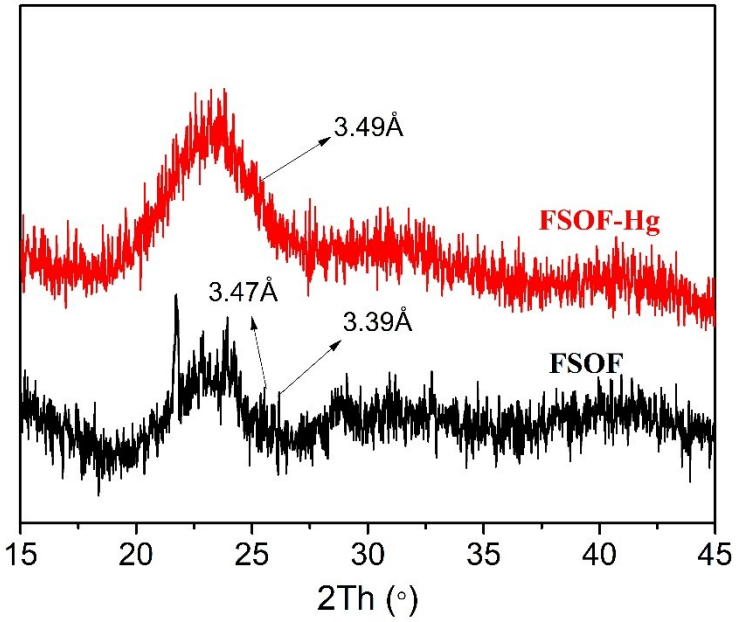

Fig. S19 The powder XRD patterns of **FSOF** and **FSOF-Hg**.

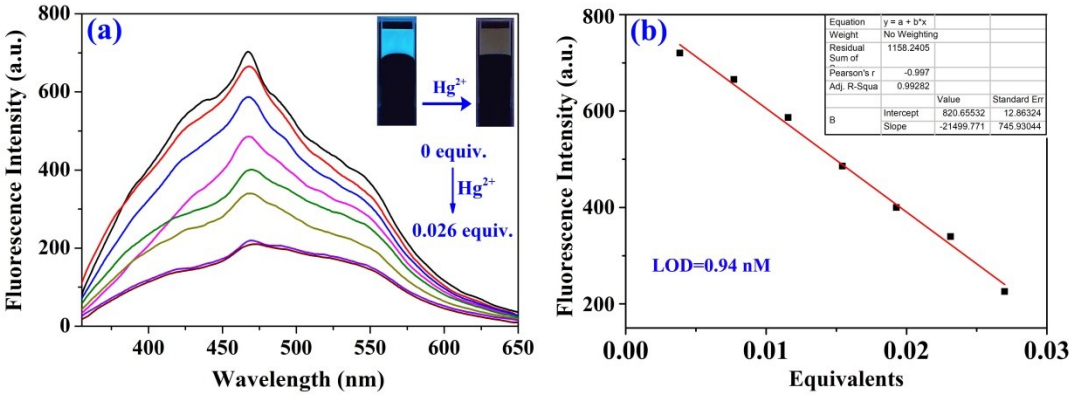

Fig. S20 (a) Emission spectra of **FSOF** with increasing amounts of Hg^{2+}; (b) photographs of the linear ranges **FSOF** for Hg^{2+}.

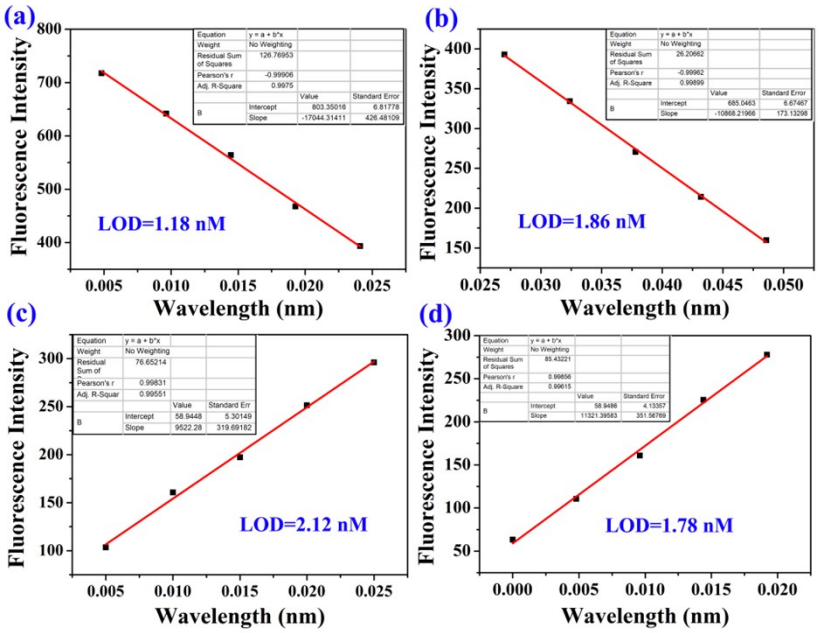

Fig. S21 Photographs of the linear ranges (a) **FSOF** for Fe^{3+}; (b) **FSOF** for Cr^{3+}; (c) **FSOF-Fe** for CN^-; (d) **FSOF-Cr** for $H_2PO_4^-$.

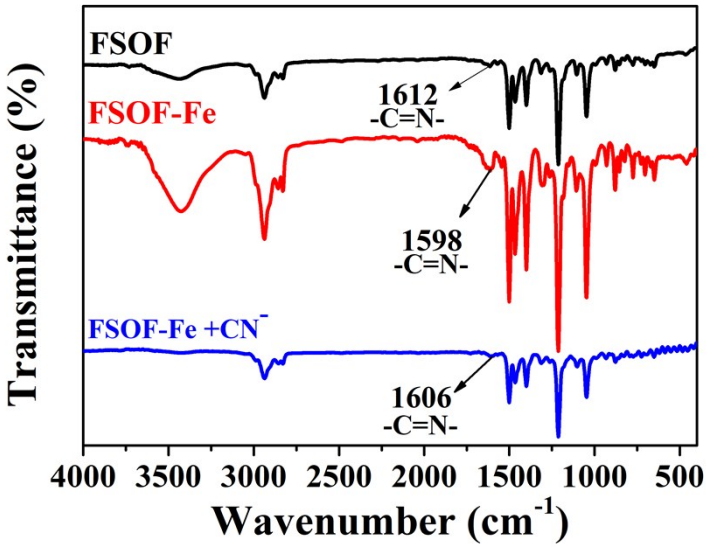

Fig. S22 FT-IR spectra of xerogel **FSOF**, **FSOF-Fe**, and **FSOF-Fe**+CN^-.

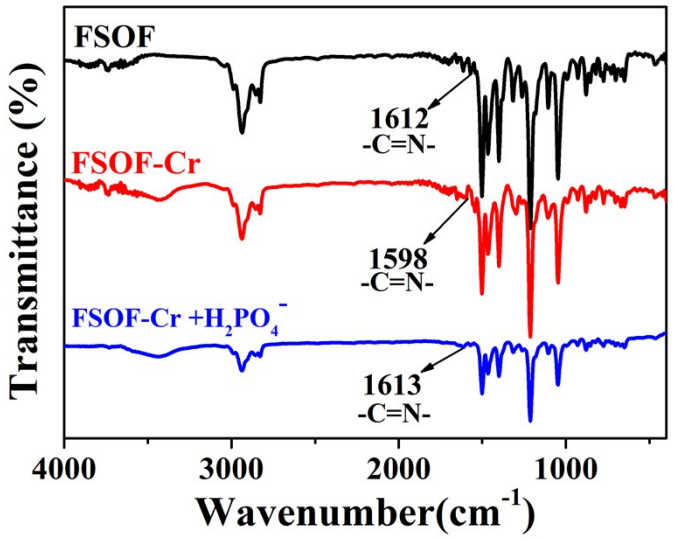

Fig. S23 FT-IR spectra of xerogel **FSOF**, **FSOF-Cr**, and **FSOF-Cr**+$H_2PO_4^-$.

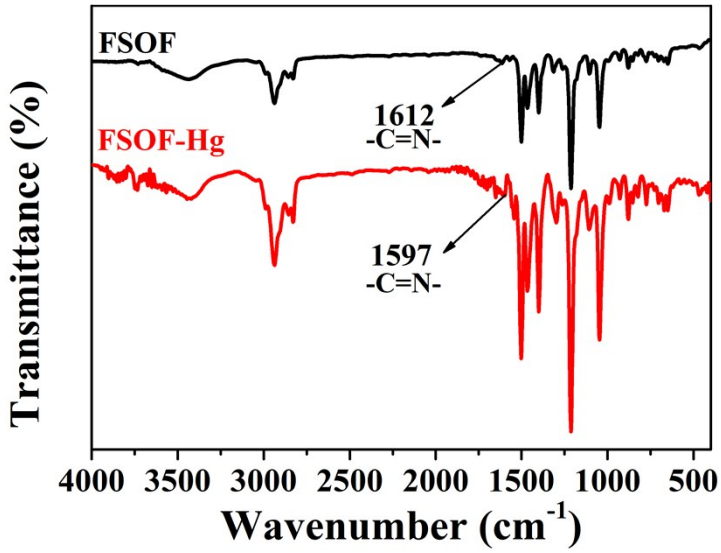

Fig. S24 FT-IR spectra of xerogel **FSOF** and **FSOF-Hg**.

Table S1. Gelation Property of tri-pillar[5]arene-based foldamer supramolecular organic framework (**FSOF**).

Entry	Solvent	State[a]	CGC[b](%)	T_{gel}[c](°C, $_{wt}$%)
1	DMSO	S	\	\
2	DMF	S	\	\
3	acetonitrile	P	\	\
4	ethanol	P	\	\
5	methanol	P	\	\
6	isopentanol	P	\	\
7	CH_2Cl_2	S	\	\
8	$CHCl_3$	S	\	\
9	ethyl acetate	S	\	\
10	THF	S	\	\
11	acetone	P	\	\
12	CCl_4	S	\	\
13	CH_2ClCH_2Cl	S	\	\
14	n-hexane	P	\	\
15	cyclohexanol	S	\	\
16	isopropanol	S	\	\
17	petroleum ether	P	\	\
18	n-butyl alcohol	G	10	50-52°C
19	n-hexanol	S	\	\
20	n-propanol	S	\	\
21	ethanediol	S	\	\
22	Tertbutylalcohol	S	\	\
23	Glycerol	S	\	\

[a] G, P and S denote gelation, precipitation and solution, respectively, c = 0.8%.

[b] The critical gelation concentration ($_{wt}$%, 10mg/ml = 1.0%).

[c] The gelation temperature (°C).

Table S2. Comparison of **the** LODs and adsorption rates of different fluorescence sensors for ions

Ions	refs	LOD(nM)
	S1	1900.00
	S2	1500
Cr^{3+}	S3	547
	S4	500
	This work	**1.86**
	S5	1300
	S6	900
Fe^{3+}	S7	23.20
	S8	1.80
	This work	**1.18**
	S9	700
	S10	30
Hg^{2+}	S11	16
	S12	3.33
	This work	**0.94**
	S13	370
	S14	170
CN^-	S15	110
	S16	50
	This work	**2.12**
	S17	3500
	S18	3000
$H_2PO_4^-$	S19	1600
	S20	900
	This work	**1.78**

References

[S1] M. Mukherjee, B. Sen, S. Pal, M. S. Hundal, S. K. Mandal, A. R. Khuda-Bukhshc, P. Chattopadhyay, *RSC Adv.* **2013**, *3*, 19978-19984

[S2] C. Dong, G. H. Wu, Z. Q. Wang, W. Z. Ren, Y. J. Zhang, Z. Y. Shen, T. H. Li, A. G. Wu, *Dalton Trans.* **2016**, *45*, 8347-8354.

[S3] E. T. Feng, C. B. Fan, N. S. Wang, G. Liu, S. Z. Pu, *Dyes Pigments* **2018**, *151*, 22-27.

[S4] M. Raju, R. R. Nair, I. H. Raval, S. Srivastava, S. Haldar, P. B. Chatterjee, *Sens. Actuators B* **2018**, *266*, 337-343.

[S5] C. Y. Zhang, J. X. Luo, L. J. Ou, Y. H. Lun, S. T. Cai, B. N. Hu, G. P. Yu, C. Y. Pan, *Chem. Eur. J.* **2017**, *24*, 3030-3037.

[S6] W. Wang, M. Wu, H. M. Liu, Q. L. Liu, Y. Gao, B. Zhao, *Tetrah. Lett.* **2019**, *60*, 1631-1635.

[S7] H. Q. Zhang, Y. H. Huang, X. H. Lin, F.F. Lu, Z. S. Zhang, Z. B. Hu, *Sens. Actuators B* **2018**, *255*, 2218-2222.

[S8] B. F. Shi, Y. B. Su, L. L. Zhang, M. J. Huang, R. J. Liu, S. L. Zhao, *ACS Appl. Mater. Interfaces* **2016**, *8*, 10717-10725.

[S9] E. Babaee, A. Barati, M. B. Gholivand, A. Taherpour, N. Zolfaghar, M. Shamsipur, *J. Hazard. Mater.* **2019**, *367*, 437-446.

[S10] M. Zhang, B. C. Yin, W. H. Tan, B. C. Ye, *Biosens. Bioelectron.* **2011**, *26*, 3260-3265.

[S11] Y. P. Zhu, T. Y. Ma, T. Z. Ren, Z. Y. Yuan, *ACS Appl. Mater. Interfaces* **2014**, *6*, 16344-16351.

[S12] H. Guo, J. S. Li, Y. W. Li, D. Wu, H. M. Ma, Q. Wei, B. Du, *Anal. Chim. Acta.* **2019**, *1048*, 161-167.

[S13] S. Momeni, R. Ahmadi, A. Safavi, I. Nabipour, *Talanta* **2017**, *175*, 514-521.

[S14] A. L. Mirajkar, L. L. Mittapelli, G. N. Nawale, K. R. Gore, *Sens Actuators B Chem.* **2018**, *265*, 257-263.

[S15] Y. Feng, D. Y. Deng, L. C. Zhang, R. Liu, Y. Lv, *Sens. Actuators B* **2019**, *279*,

189-196.

[S16] Y. Y. Feng, L. Shi, H. S. Wu, L. C. Chen, Y. W. Chi, *Electrochim. Acta.* **2018**, *261*, 29-34.

[S17] X. J. Meng, S. l. Li, W. B. Ma, J. L. Wang, Z. Y. Hu, D. L. Cao, *Dyes Pigments* **2018**, *154*, 194-198.

[S18] V. Bhalla, V. Vij, M. Kumar, P. R. Sharma, T. Kaur, *Org. Lett.* **2012**, *14*, 1012-1015.

[S19] S. Sen, M. Mukherjee, K. Chakrabarty, I. Hauli, S. K. Mukhopadhyayc, P. Chattopadhyay, *Org. Biomol. Chem.* **2013**, *11*, 1537-1544.

[S20] H. D. Duong, J. I. Rhee, *Sens Actuators B* **2018**, *274*, 66-77.